Supporting Information: Dynamic behavior of the single-strand DNA molecules from the hydrophilic to hydrophobic regions on graphene oxide surface driven by heating

Mengjiao Wu[1], Yingying Huang[1], Li Yang[2], Yongshun Song[1,*] and Xiaoling Lei[1,*]

1 School of Physics, East China University of Science and Technology, Shanghai 200237, China.
2 College of Physics Science and Technology, Guangxi Normal University, Guilin 541004, China

1. The multi-sample simulations

At the beginning of our simulation, we conducted tests on temperature at 320 K,

350 K and 400 K respectively to determine the proper temperature in our simulation. The simulation systems were constructed as Table S1.

Table S1. Detail of various systems simulated in this study.

Length of ssDNA (mer)	Number of samples	Temperature (K)	Simulation time (ns)	Number of samples from hydrophilic to hydrophobic regions
4	4	320	400+120	0
	4	350	400	2
	4	400	400	2
8	4	320	400+120	0
	4	350	400	2
	4	400	400+120	2

We constructed four different initial conformations on GO surface for 4-mer and 8-mer ssDNA, of which each was initially run for 400 ns at 320 K, 350 K and 400 K, respectively. At 320 K, no ssDNA molecules moved from the hydrophilic to hydrophobic regions on the GO surface by heating from 300 K for either the 4-mer or 8-mer ssDNA. At 350 K, sample 2 and sample 3 for the 4-mer and 8-mer ssDNA, respectively, moved from the hydrophilic to hydrophobic regions on the GO surface by heating. At 400 K, sample 2 and sample 3 for the 4-mer ssDNA and sample 2 for the 8-mer ssDNA moved from the hydrophilic to hydrophobic regions on the GO surface by heating. Then we extended the simulation time from 400 ns to 520 ns for the samples at 320 K and 400K which did not achieve ssDNA molecule's regional changing from hydrophilic to hydrophobic regions on GO surface, which simulation results as shown in Figure S1. Finally, at 520 ns, there is still no ssDNA molecules moved from hydrophilic to hydrophobic regions on the GO surface by heating for either the 4-mer or 8-mer ssDNA at 320 K; and sample 3 for 8-mer ssDNA achieved regional changes from hydrophilic to hydrophobic regions on GO surface at 400 K. Obviously, even extending the simulation time from 400 ns to 520 ns, it is still difficult to drive ssDNA from the hydrophilic to hydrophobic regions by heating from 300 K to 320 K. At 400 K, it takes a longer simulation time to achieve the same probability of ssDNA molecule

moved from the hydrophilic to hydrophobic regions by heating as at 350K. Therefore, we chosen 350 K as the simulation temperature to investigate the dynamic behavior of the ssDNA on the GO surface driven by heating.

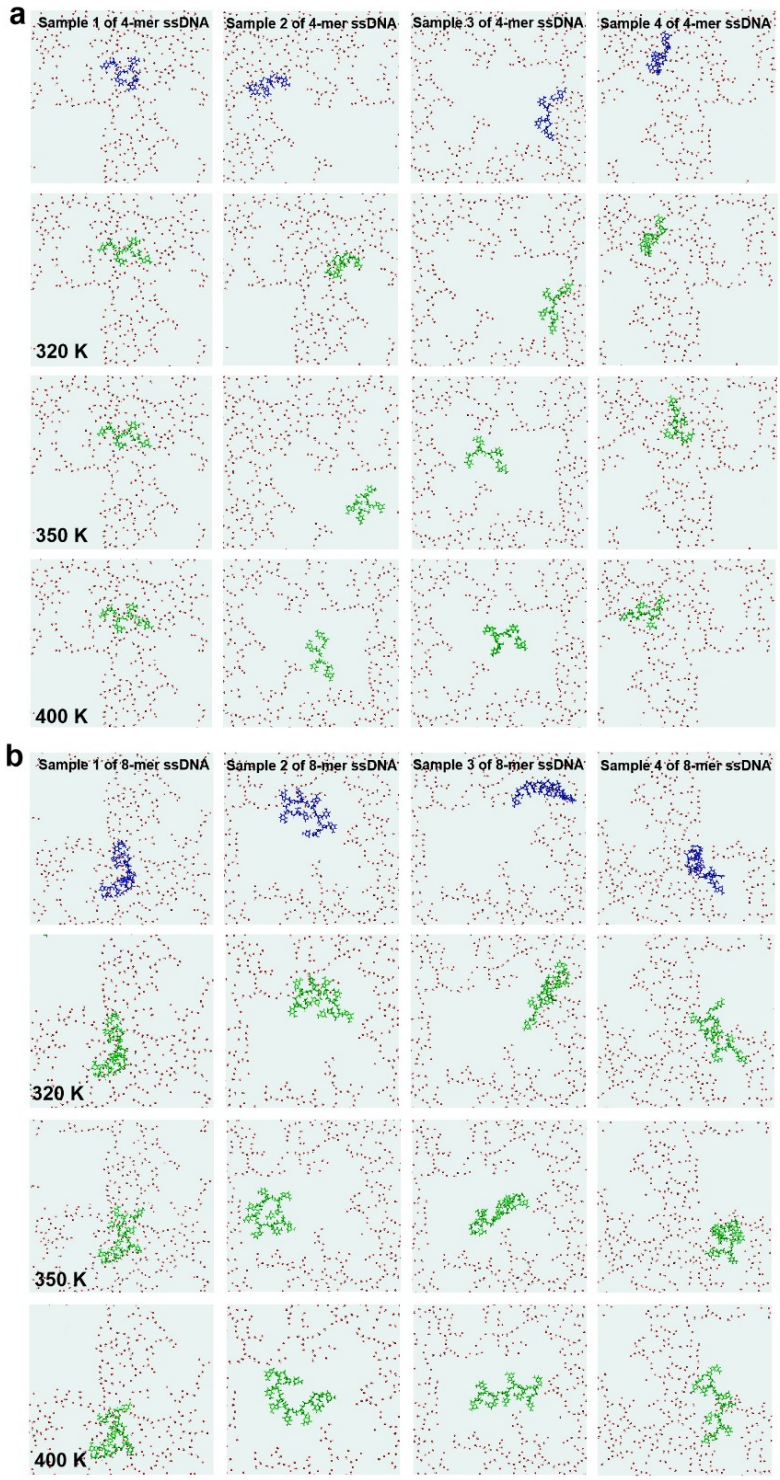

Figure S1. Snapshots of all samples of (a) 4-mer and (b) 8-mer ssDNA on the GO surface. Blue chain: the initial site of ssDNA on GO surface. Green chain: the final site of ssDNA on GO surface at 320 K, 350 K and 400 K, respectively. The oxygen and hydrogen atoms in the GO surface were shown by red spheres and white spheres, respectively.

2. The GO model

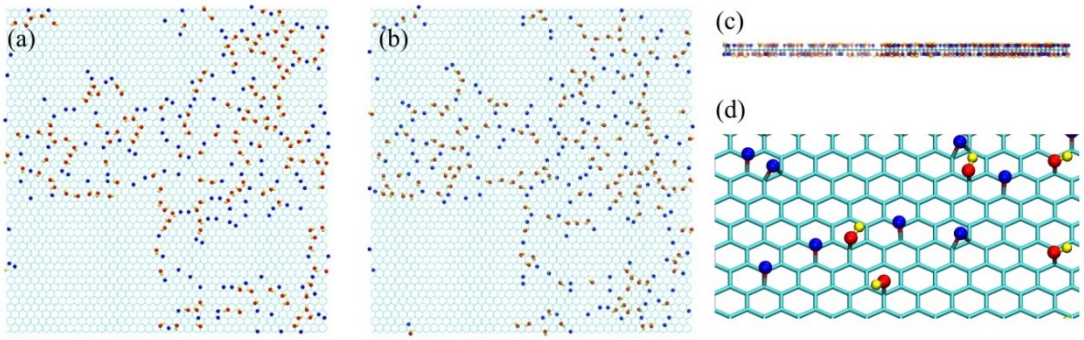

Figure S2 (a), (b), (c) and (d) are top, back, side and local views of the GO nanosheet used in our simulation.

The GO nanosheet was constructed based on the Shi-Tu structure model[1] with a formula of $C_{10}O_1(OH)_1(COOH)_{0.5}$[2-4]. The size of the GO nanosheet is 10.084 nm × 10.224 nm, and the GO nanosheet contains 311 hydroxyl groups (-OH) and 290 epoxy groups (-O-), where the distribution of functional/oxidized groups on GO is generated according to the rate-constant ratios from the computation by combining density functional theory with conventional transition-state theory and the oxidation loci on GO is highly correlated, which is consistent with recently experimental observations [5-11]. This high correlation leads to the coexistence of both large unoxidized and oxidized regions on GO. The correlation length is 4.2 ± 0.5 nm. More importantly, in oxidized regions on GO, there are some small areas of sp^2-hybridized domains that we called 'island' region as shown in Figure S2. Based on the correlations, the size of the patch islands was estimated to be up to 0.65 ± 0.03 nm.

The detailed force field parameters of GO can be referred to our previous publication[5, 6]. Briefly, carbon atoms are modeled as uncharged Lennard-Jones particles with a cross-section of σ_{CC} = 3.58 Å and a depth of potential well ε_{CC} = 0.0663 kcal mol^{-1} [6, 12, 13]. The C-C bond length of 0.142 nm, C-C-C bond angle of 120°, and C-C-C-C planar dihedral angles, are maintained by harmonic potentials with spring constants of 322.55 kcal mol^{-1} $Å^{-2}$, 53.35 kcal mol^{-1} rad^{-2} and 3.15 kcal mol^{-1}, respectively. The OH group is vertical to the plane with the C-O bond length of 1.36 Å, O-H bond length of 1.0 Å, O-C-C (graphene) bond angle of 90°, H-O-C bond angle of

109.5°. The parameter of epoxy is the C-C bond length of 1.481 Å, C-O-C bond angle of 57.3°, O-C-C bond angle of 61.35°, and O-C-C (graphene) bond angle of 103.90°.

3. Snapshots of ssDNA on GO surface.

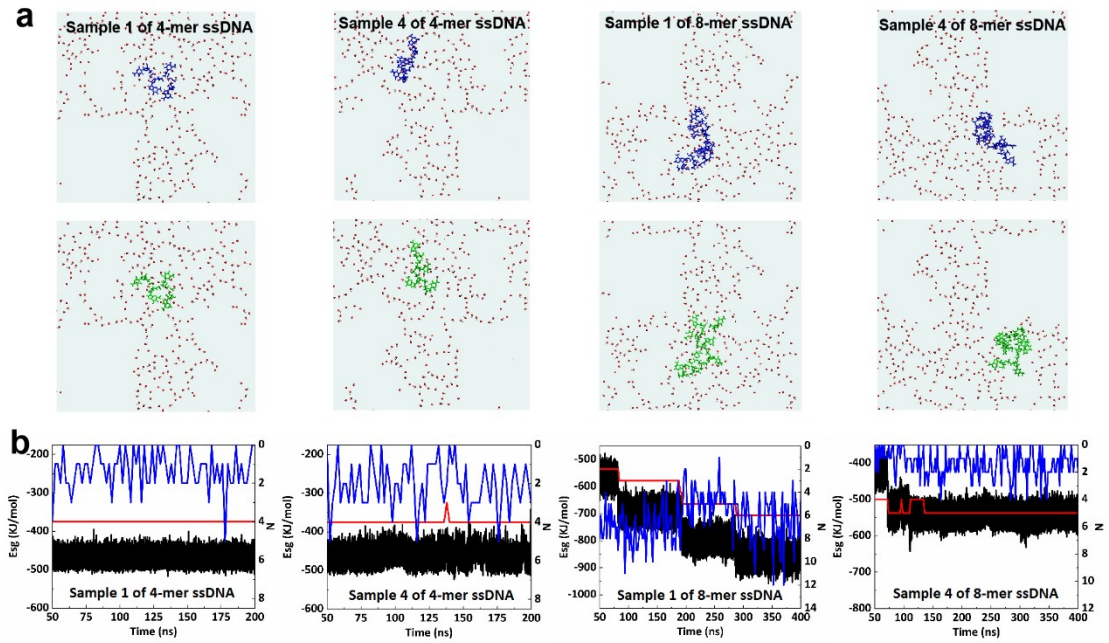

Figure S3. Snapshots of ssDNA on the GO surface at 350 K. Blue chain: the initial conformation of ssDNA on GO surface. Green chain: the final conformation of ssDNA on GO surface during simulation time. The oxygen and hydrogen atoms in the GO surface were shown by red spheres and white spheres, respectively. (b) Time evolution of interaction energy between ssDNA molecules and the GO surface at 350 K. Black curve: Esg; red curve: the number of π-π stacking structures between the ssDNA molecule and the GO surface; blue curve: the number of hydrogen bonds between the ssDNA molecule and the GO surface

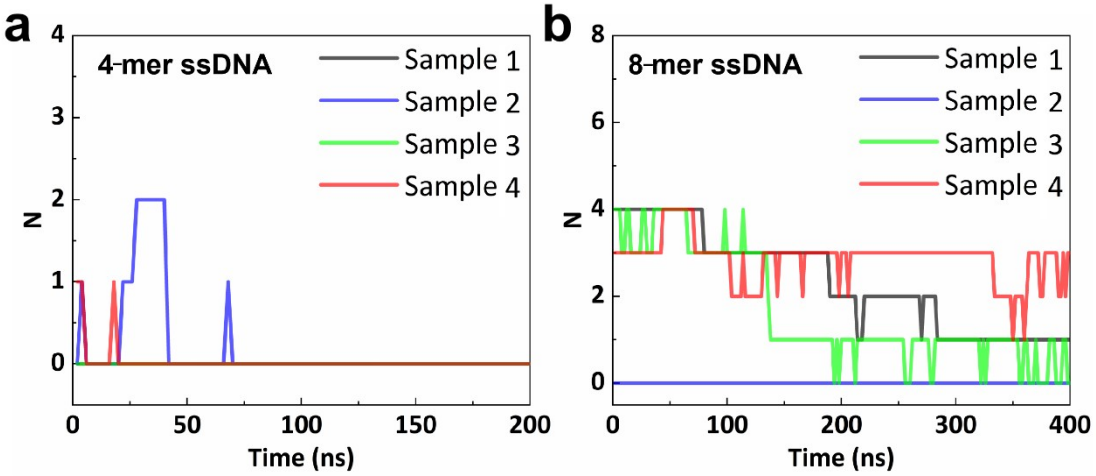

4. The number of intra π-π stacking structure of ssDNA molecule.

Figure S4. The number of intra π-π stacking structure of ssDNA molecules on the GO surface at 350 K.

5. The end-to-end distance of ssDNA molecules on GO surface

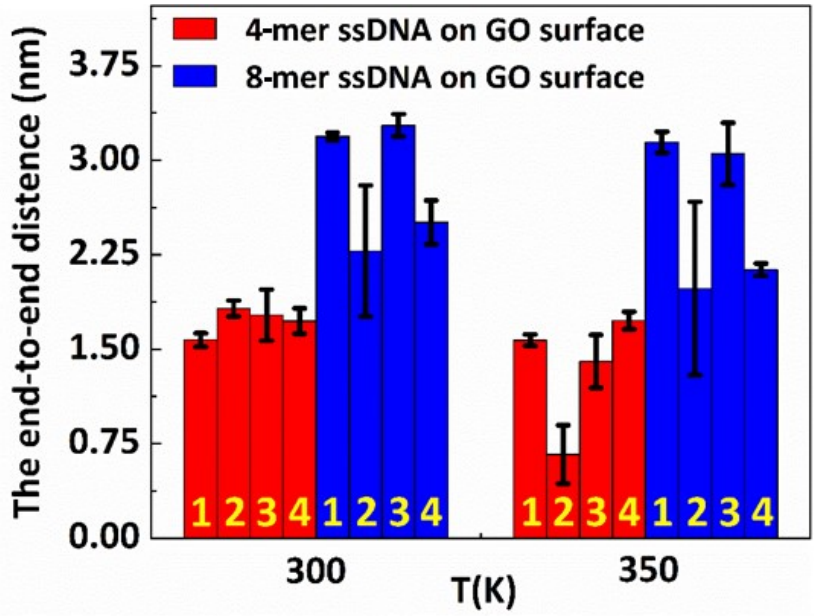

Figure S5. The average end-to-end distance of ssDNA molecules on GO surface were measured during the last 20 ns. The sample IDs were indicated in the figure.

6. The dynamic behavior of sample 3 of 8-mer ssDNA from the hydrophilic to hydrophobic regions on GO surface.

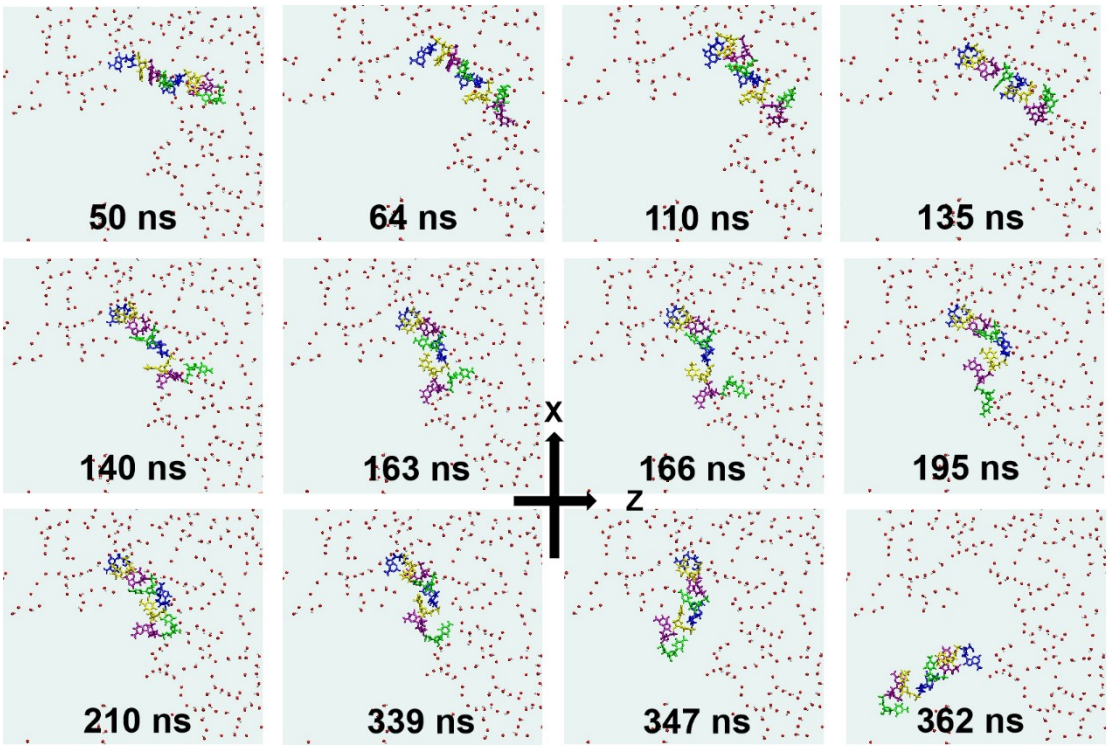

Figure S6. Snapshots of sample 3 of 8-mer ssDNA from the hydrophilic to hydrophobic regions on GO surface at 350 K. The adenosine, thymidine, guanosine and cytidine of the ssDNA molecule were shown by blue, yellow, purple and green, respectively.

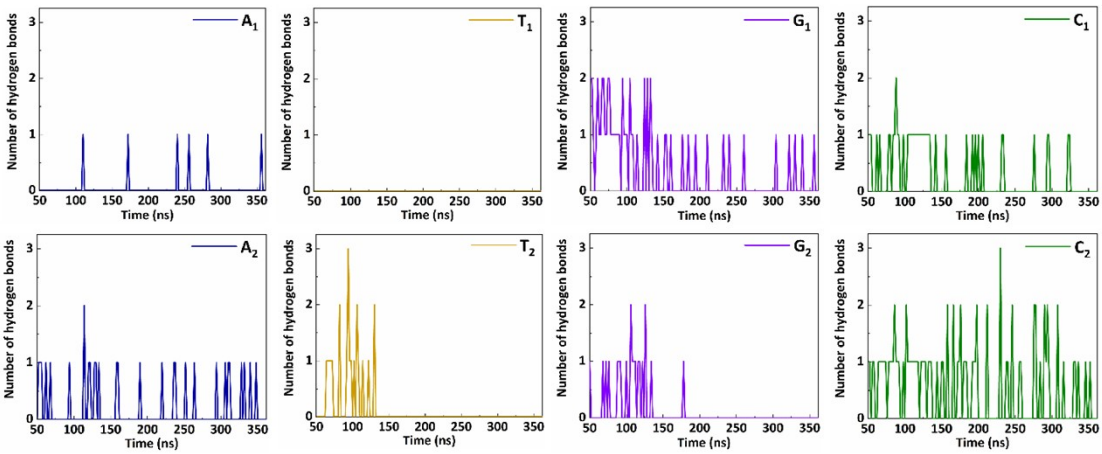

Figure S7. The number of hydrogen bonds between adenosine (A_1 and A_2), thymidine (T_1 and T_2), guanosine (G_1 and G_2) and cytidine (C_1 and C_2) and the GO surface at 350 K. The data were collected every 2 ns.

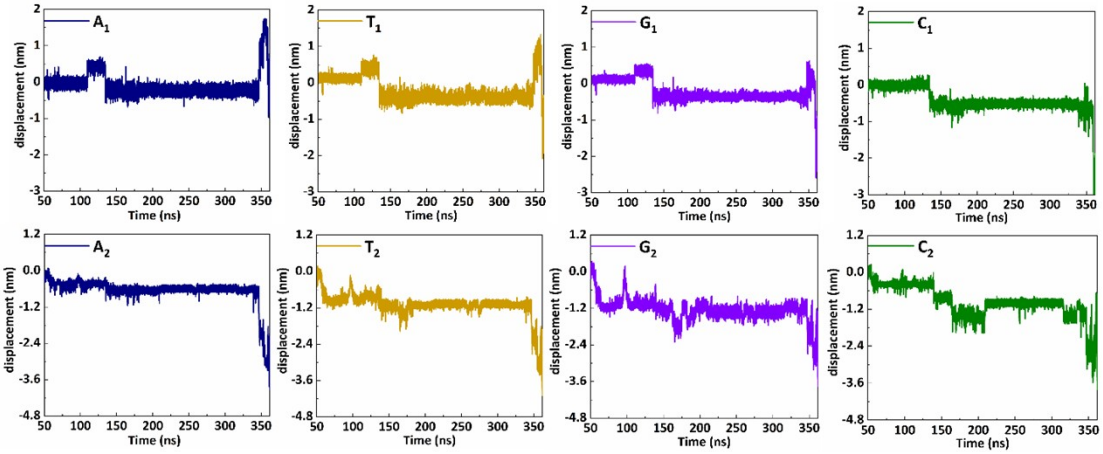

Figure S8. Time evolution of centroid displacement for adenosine (A_1 and A_2), thymidine (T_1 and T_2), guanosine (G_1 and G_2) and cytidine (C_1 and C_2) of 8-mer ssDNA molecule on the GO surface at 350 K. The data were collected from 50 ns to 362 ns.

To fully understand the dynamic process, we presented detailed snapshots of sample 3 of 8-mer ssDNA molecule moving from the hydrophilic to hydrophobic regions at 350 K as shown in Figure. S6. The dynamic process is analyzed along with the number of hydrogen bonds between different nucleosides (adenosine A_1 and A_2, thymidine T_1 and T_2, guanosine G_1 and G_2 and cytidine C_1 and C_2) and the GO surface, as shown in Figure S7. At about 64 ns, the number of hydrogen bonds between T_2, G_2 and the GO surface increase from 0 to 1 as shown in Figure S7. This leads to the centroid displacement for T_2 and G_2 respectively changes about 1.2 nm as shown in Figure S8 and moves into the adjacent sp^2 hybridized regions as shown in Figure S6. At the same time, the A_2 and C_2 are dragged towards hydrophobic regions, causing centroid displacement changes of about 0.60 nm, respectively. At about 110 ns, the number of hydrogen bonds between A_1 and the GO surface increase from 0 to 1 as shown in Figure S7. Meanwhile the number of hydrogen bonds between G_1 and the GO surface increase from 0 to 2. This leads to the centroid displacement for A_1 and G_1 changes about 0.5 nm, respectively, as shown in Figure S8, further making G_1 forms 1 intra π-π stacking structure with T_1, which increases the number of intra π-π stacking structures from 3 to 4 as shown in Figure S4b. Therefore, the number of hydrogen bonds between T_1 and the GO surface is always zero. Meanwhile this behavior changes the

G_1 balanced interactions and destroys the stable structure. Therefore, the G_1 constantly adjusts its structure through a competition between intra and inter π-π stacking structures to balance the external hydrogen bonds interactions. At about 135 ns, the G_1 forms 1 inter π-π stacking structure with the hydrophobic regions of GO surface, which decreases the number of intra π-π stacking structures from 4 to 3 as shown in Figure S4b. This leads to the centroid displacement for G_1 changes about 1.0 nm as shown in Figure S8. At the same time, the A_1, T_1, C_1, A_2, T_2 and C_2 are dragged towards hydrophobic regions and their number of hydrogen bonds with the GO surface decrease to 0, respectively, as shown in Figure S7. It is worth emphasizing that the A_1, T_1, G_1, C_1, A_2 and T_2 are totally in the hydrophobic regions. Due to the hydrophobic regions is very smooth, the sliding behavior of nucleobases will affect the behavior of DNA on the GO surface and drags DNA into the hydrophobic region as shown in Figure S6 at 140 ns. To further release the structure stress, the G_2 and T_2 continue to move towards the hydrophobic regions. At 163 ns, the T_2 forms 1 inter π-π stacking structures with the GO surface, and the centroid displacement changes about 0.5 nm as shown in Figure S8. At the same time, the adenosine, guanosine and cytidine are dragged towards hydrophobic regions, causing centroid displacement changes. The sliding behavior of T_2 and G_2 will affect the behavior of ssDNA on the GO surface and drags ssDNA into the hydrophobic region as shown in Figure S6 at 166 ns-210 ns. Afterwards, the sliding behavior of T_2, G_2 and C_2 continue to drag the other nucleotides towards the hydrophobic regions as shown in Figure S6 at 339 ns-347 ns. Finally, at 362 ns, the ssDNA totally moves into the hydrophobic regions.

References

1. J. Yang, G. Shi, Y. Tu and H. Fang, High correlation between oxidation loci on graphene oxide, *Angew. Chem. Int. Ed. Engl.*, 2014, **53**, 10190.
2. A. Lerf, H. He, M. Forster and J. Klinowski, Structure of Graphite Oxide Revisited‖, *J. Phys. Chem. B,* 1998, **102**, 4477.
3. N. Medhekar, A. Ramasubramaniam, R. Ruoff and V. Shenoy, Hydrogen Bond Networks in Graphene Oxide Composite Paper: Structure and Mechanical Properties, *ACS Nano*, 2010, **4**, 2300.
4. C. Shih, S. Lin, R. Sharma, M. Strano and D. Blankschtein, Understanding the pH-dependent behavior of graphene oxide aqueous solutions: a comparative experimental and molecular dynamics

simulation study, *Langmuir*, 2012, **28**, 235.

5. Y. Tu, M. Lv, P. Xiu, T. Huynh, Q. Huang, C. Fan, M. Zhang, H. Fang and R. Zhou, M. Castelli, Z. Liu, Destructive extraction of phospholipids from Escherichia coli membranes by graphene nanosheets, *Nat. Nanotechnol.*, 2013, **8**, 594.
6. H. Geng, X. Liu, G. Shi, G. Bai, J. Ma, J. Chen, Z. Wu, Y. Song, H. Fang and J. Wang, Graphene Oxide Restricts Growth and Recrystallization of Ice Crystals, *Angew. Chem. Int. Ed. Engl.*, 2017, **56**, 997.
7. D. Chen, H. Feng and J. Li, Graphene oxide: preparation, functionalization, and electrochemical applications, *Chem. Rev.*, 2012, **112**, 6027.
8. D. Dreyer, S. Park, C. Bielawski and R. Ruoff, The chemistry of graphene oxide. *Chem Soc Rev*, 2010, **39**, 228.
9. W. Cai, R. Piner, F. Stadermann, S. Park, M. Shaibat, Y. Ishii, D. Yang, A. Velamakanni, S. An, M. Stoller, J. An, D. Chen and R. Ruoff, Synthesis and solid-state NMR structural characterization of ^{13}C-labeled graphite oxide, *Science*, 2008, **321**, 1815.
10. J. Meyer, C. Girit, M. Crommie and A. Zettl, Imaging and dynamics of light atoms and molecules on graphene, *Nature*, 2008, **454**, 319.
11. K. Erickson, R. Erni, Z. Lee, N. Alem, W.Gannett and A. Zettl, Determination of the local chemical structure of graphene oxide and reduced graphene oxide, *Adv. Mater.*, 2010, **22**, 4467.
12. A. Titov, P. Král and R. Pearson, Sandwiched Graphene-Membrane Superstructures, *ACS Nano*, 2010, **4**, 229.
13. N. Patra, B. Wang and P. Král, Nanodroplet Activated and Guided Folding of Graphene Nanostructures, *Nano Lett.*, 2009. **9**, 3766.